Bond Graph Modeling, Simulation, and Control of Permanent Magnet Linear Synchronous Motor

PMLSM Motor Based EVs Applications

Aminu BABANGIDA
Department of Mechatronics
Faculty of Engineering
University of Debrecen
Debrecen, Hungary
aminubabangida24@gmail.com

Géza HUSI
Department of Mechatronics
Faculty of Engineering
University of Debrecen
Debrecen, Hungary
husigeza@eng.unideb.hu

Pèter Tamás SZEMES
Department of Mechatronics
Faculty of Engineering
University of Debrecen
Debrecen, Hungary
szemespeter@eng.unideb.hu

Abstract— **The high-performance feature of the Permanent Magnet Linear Synchronous Motor (PMLSM) makes it a reliable and valuable motor for use in the automotive industry, especially for electric vehicle (EVs) applications. This research proposes a bond graph approach in modeling the PMLSM as a multi-domain dynamical system.**

However, A time-based simulation was performed using 20-sim software to simulate the dynamical behavior of the motor. An equivalent model of the motor was first obtained and then modeled and simulated using 20-sim software. The model of the PMLSM drive system was modeled separately and incorporated with PMLSM Motor equivalent model to form a global model.

Moreover, the motor drive system response was studied based on the sensor resolutions and the inverter switching frequency. The block diagram and the transfer function methods validated the bond graph model obtained. Two classical PIs such as continuous and discrete were implemented on the motor response to control the velocity of the motor.

Keywords—Bond graph, EVs, PMLSM Motor, PIs, 20-sim

I. INTRODUCTION

The high accuracy, speed, and power density of the PMLSM make it a suitable electrical motor in industrial applications such as semiconductor manufacturing equipment. Its high speed, energy-saving, and reliability features make it an excellent motor EV application. The simple structure of this type of motor is its simple structure. "Direct drive system with linear motor, compared with traditional indirect drive system which consists of a rotary motor with a ball-screw transmission to the slide, can have a high positioning accuracy, high speed, high acceleration, and fast responding" [1]. Another study pointed out that linear motors, in general, can transfer the force applied on a moving body without using a mechanical means, i.e., transmission [2]. Further study in [3] emphasized the advantages of linear motors over conventional motors, such as shorter response time, higher precision for positioning, etc. However, a

PMLSM is considered a mechatronics engineering system that integrates the sensor, the motor drive system, the controller, and the mechanical part [4]. Therefore, the performance of the PMLSM motor depends on the electrical and kinematic parameters. A multi-domain approach such as a bond graph is adopted in this research to model the PMLSM motor and its drive. The bond graph is considered as a powerful tool for modeling the dynamical behavior of the physical systems. "It enhances the visual understanding of these systems through the visual indication of the cause-and-effect relationships of the energy transfer between the subsystem variables" [5]. A bond graph has been a tool used by many researchers for capturing the typical energy of the physical systems with multi-domain structures such as electrical, mechanical, thermal, fluid, and many other systems. For example, V. Anan et al. in[6] performed bond graph modeling and simulation of the permanent magnet brushless DC motor. According to the research, the bond graph method has been proposed because it increases the insight into studying the system's behavior in question. More so, the bond graph is a modeling approach for complex systems. In [7], the bond graph has been applied in various disciplines, including all engineering aspects, and of course like biological systems. M. Teodor et al. in [8] their study of the bond graph modeling and simulation of the Permanent DC Motor (PMDC) stated that with bond graph, any complex system can be analyzed as unique system and any physical measure can be determined easily.

A review works of the literature shows that many have applied the bond graph approach in modeling multi-domain systems, including engineering and biological systems like [9], [10], [11], [12], [13], and [14]. For example, M. Asif in [9] researched a theoretical framework for modeling and simulation with optimal control systems of voluntary biomechanical systems. In his research, he applied the bond graph method for modeling physical systems concerning the human body. Another study in [10] performed DNA analysis using the bond graph modeling approach. Global perspective-

based bond graph and memristor methods of the DNA description system were proposed. The study concluded that the technique applied demonstrated the procedure is quite systematic and reliable in describing the dynamical behavior of the DNA system.

Nevertheless, another analysis in [11] investigated bond graph modeling and PID linearization of a single model. The study proposed a multi-domain biomechanical system forming a complex system, where a bond graph method was employed to describe the system dynamics. A 20-sim software was presented as a simulation environment. A similar study in [12] proposed a bond graph approach for modeling and analysis of physiological motor. A bond graph for the musculoskeletal feedback systems was obtained with a linear H2 optimal controller for the analysis of the parameters of different physiological systems. The study in [13] has presented modeling of anthropomorphic prosthetics using the bond graph method. With the bond graph model, the state-space model was obtained for the purpose of analysis. Further study in [14] has presented electrical power analysis using a scattering bond graph. In this study, the active and reactive power of the power system were obtained using bond graph analysis.

The remainder of this research is organized as follows: in section II, the bond graph modeling approach is described. The paper objectives and its research novelty, the power variables, the causality, and different physical domain variables are discussed. In section III, the mathematical, the bond graph models of the PMLSM motor, the model validation were described. The motor drive's bond graph model is discussed in section IV, and sections V and VI have presented the simulation results and conclusion, respectively.

II. THE BOND GRAPH APPROACH

A bond graph is a multi-domain modeling approach used for any physical system. The bond graph is used for modeling complex systems consisting of different structures. It is used for modeling electrical system systems such as RLC circuits, mechanical systems such as mass-spring-damper systems, hydraulic systems, and many more. Dynamical systems consisting of energy can be represented as bond graph models, and the model's behavior with differential-algebraic equations can be obtained by the well-established algorithms [15]. Bond graph considers the energy flows between the ports of the engineering components [16]. Suppose the concept of the bond graph is correctly established on the system dynamics. In that case, it follows the principle of the energy of conservation without reformulating the mathematical equation from scratch. The power bond in the bond graph represents the energy flow between them [16]. There are nodes called power ports in the bond graph through which an energy enters or leaves [16]. The software supporting bond graph modeling is the 20-sim proposed in this study to model and simulate the PMLSM motor and its drive.

A. Bond graph Causality

After a successful bond graph model of the system, the next stage is to assign the causality on the model. The causality is used to indicate the direction of effort and flow on the bond graph model.

B. The Power Variables

Power is the generalized coordinate for modeling coupled systems in different domains. For example, in a situation where the electrical motors are connected to hydraulic or thermal systems. Therefore, this power is defined as the product of the two conjugate variables: effort (e) and flow (f) [16].

$$Power = Effort \times Flow \qquad (1)$$

In bond graph modeling, there are some connection analogies bond graph elements that are used. For example, the **Se** is used to denote the source of effort, which represents an ideal source of voltage or force applied in electrical and mechanical domains. The **Sf** means the flow source, representing an ideal current or applied velocity source in electrical and mechanical domains. **R**, **C**, and **I** represent the electrical resistor or damper, capacitor or spring, and Inertia or mass, respectively [17]. Fig. 1 depicts the energy flow represented by a half arrow called the bond, associated with the variables: effort and flow, and the direction of flow is indicated by the causality.
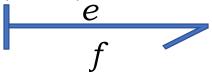

Fig. 1 Bong graph Causality Convention

The power equation of the above figure can be represented by equation 2 below:

$$p = e \times f \qquad (2)$$

TABLE I.   MAIN PHYSICAL DOMAINS VARIABLES [5]

Physical domain	Flow	Effort
Electrical	Current	Voltage
Mechanical	Velocity	Force
Hydraulic	Volume flow	Pressure
Thermal	Entropy flow	Temperature

Table I above shows the main physical domains variables used in various engineering systems.

However, this paper is aimed to precisely achieve the following goals:

- ➢ Mathematical Description of the PMLSM based Vector Control and its approximation to an equivalent circuit model.
- ➢ Bond graph modeling and simulation of the equivalent circuit of the PMLSM from the Vector Control approximation in 20-sim software.
- ➢ Validation of the bond graph model.
- ➢ Bond graph modeling and description of the PMLSM drive (Power electronics) and simulation in 20-sim.

- ➤ Bond graph modeling and simulation of the PMLSM motor and its drive in 20-sim.
- ➤ Implementation of the two classical PIs to control the motor output velocity.

Furthermore, this paper has significantly made the following contributions:

- ➤ Comparative analysis on the performance of two classical controllers for the motor velocity control.
- ➤ Validation of the motor dynamical model using the bond graph model approach.
- ➤ Analysis of the motor drive response based on sensor resolutions and inverter switching frequency.

Nevertheless, the high-performance application as in electric cars requires an efficient electric motor for better propulsion of the vehicle. The application of electrical motors, in general, is not limited, particularly for electric and hybrid cars, due to the drive system's practical design and robustness, especially the inverter. Without it, the applications of electrical machines would be limited. Therefore, the novelty of this research is despite the conventional electromagnetic transformation as in other electrical machines; the study has considered signal processing and analysis using sensor resolutions and inverter switching frequency. The higher the switching frequency, the faster the response would be.

III. THE PMLSM MOTOR

The linear motors are used to produce linear motion [18]. There are no motion translators such as gears, belts, and ball screws as in the rotation motors, making linear motors less complex and limited [19]. Therefore, a PMLSM motor is an electric motor that converts electrical energy into linear movement without a transmission mechanism. PMLSM motors are increasingly used by automotive industries in actuators, electric vehicles propulsions, robots, etc. [20]. Fig.2 indicates a simple sketch of the PMLSM motor as adapted.
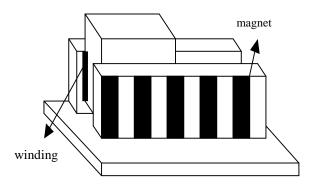

Fig. 2 PMLSM Motor [2]

A. PMLSM Mathematical Model

The mathematical model of the PMLSM motor is derived from the rotary Permanent Magnet Synchronous Motor (PMSM) model based on the fundamental theory of electrical machines [21]. To model the motor, the following assumptions were made as studied in [21] as follows:

- ➤ The three-phase windings are symmetrical, star connected.
- ➤ There are linear magnetizing characteristics.
- ➤ Zero loss in the magnetic circuit.
- ➤ Constant resistances, inductances, and air gaps.
- ➤ Sinusoidal distribution of the magnetic field in the air gap.
- ➤ Constant longitudinal axis, and
- ➤ Boundary effects and grooves influence are neglected.

However, the coordinate system of the motor as shown in fig. 3, where the model is described in d-q coordinate system.
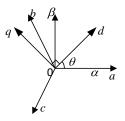

Fig. 3 Coordinate System [21]

Therefore, the following matrix equation is obtained according to the unified theory of electrical machines [21]:

$$C_{3s/2s} =$$
$$\sqrt{\frac{2}{3}} \cdot \begin{pmatrix} cos\theta & cos(\theta - \frac{2}{3}\pi) & cos(\theta + \frac{2}{3}\pi) \\ -sin\theta & -sin(\theta - \frac{2}{3}\pi) & -sin(\theta + \frac{2}{3}\pi) \\ \frac{1}{\sqrt{2}} & \frac{1}{\sqrt{2}} & \frac{1}{\sqrt{2}} \end{pmatrix} \quad (3)$$

Therefore, the voltages equation in the d-q axis is as follows:

$$\begin{pmatrix} U_d \\ U_q \\ U_0 \end{pmatrix} =$$
$$\sqrt{\frac{2}{3}} \cdot \begin{pmatrix} cos\theta & cos(\theta - \frac{2}{3}\pi) & cos(\theta + \frac{2}{3}\pi) \\ -sin\theta & -sin(\theta - \frac{2}{3}\pi) & -sin(\theta + \frac{2}{3}\pi) \\ \frac{1}{\sqrt{2}} & \frac{1}{\sqrt{2}} & \frac{1}{\sqrt{2}} \end{pmatrix} \cdot \begin{pmatrix} U_a \\ U_b \\ U_c \end{pmatrix} \quad (4)$$

U_d and U_q are the voltage components in the d-q axis

The following equation describes the voltage equation in d-axis:

$$L_d \frac{di_d}{dt} + R. i_d = U_d + \frac{\pi}{\tau}. V. L_q. i_q \quad (5)$$

The voltage equation in the q-axis is described as follows:

i_d and i_q are the current components in the d-q axis

$$L_q \frac{di_d}{dt} + R.i_q = U_q + \frac{\pi}{\tau}.V.L_d.i_d - \psi_f.\frac{\pi}{\tau}.v \qquad (6)$$

L_q and L_d are d-q axis inductances, ψ_f is the permanent magnet flux linkage, and R, the resistance of the windings.

The following equation gives the electromagnetic thrust force:

$$F_e = \frac{3\pi}{2\tau} N_p (\psi_f i_q + (L_d - L_q) i_q i_d) \qquad (7)$$

Where N_p is the number of pole pair

And the dynamical equation of the PMLSM is described as follows:

$$M \frac{dv}{dt} = F_e - F_d - B_v v \qquad (8)$$

Where F_d, M, B_v Are the external force, moving part mass, and viscous friction.

And the velocity is given by the following equation:

$$v = 2\tau f \qquad (9)$$

Where f is the motor frequency, and τ is pole-pitch

B. Bond Graph Model of the PMLSM

Using field-oriented control strategy, assuming $i_d = 0$, then the force of the motor is proportional to the i_q, therefore, the PMLSM can be treated as a DC motor, and the equivalent circuit model is as shown in fig. 4 below [4]:
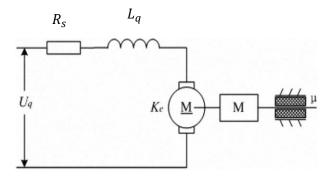

Figure 4 PMLSM Equivalent Circuit Model [4]

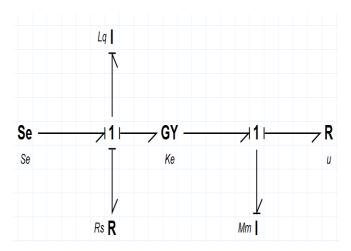Using the 20-sim, the bond graph model can be obtained as:

Fig. 5 20-sim Simulation of PMLSM Equivalent Model

To obtain the power flow, each bond on the bond graph of fig. 5 is numbered, each representing the effort and the flow as shown in the figure below:
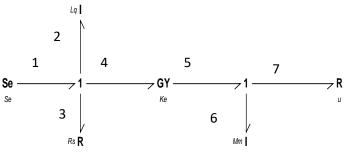

Fig. 6 Bond Graph Model of PMLSM

From the bond graph model of the PMLSM motor in Fig. 6 above, Se is the input voltage, $I: Lq$ is the Inductance, $R: Rs$ is the series resistance, $I: Mm$ is the slider mass, GY is the gyrator, which denotes the energy conversion between the magnetic and mechanical energy, Ke is the conversion coefficient, and u is the constant [4]. Therefore, the state-space model can be described as in [1] as follows:

$$p_2 = f_2 L_q \qquad (10)$$

$$p_6 = f_6 M \qquad (11)$$

$$e_3 = R_s f_3 \qquad (12)$$

$$e_7 = \mu f_7 \qquad (13)$$

$$f_1 = f_2 = f_3 = f_4 \qquad (14)$$

$$e_1 = e_2 + e_3 + e_4 \qquad (15)$$

$$f_5 = f_6 = f_7 \qquad (16)$$

$$e_5 = e_6 + e_7 \qquad (17)$$

$$e_5 = K_e f_4 \qquad (18)$$

$$e_4 = K_e f_5 \qquad (19)$$

Where e_i and f_i (for $i = 1, 2, 3 \dots 7$) are effort and flow on each of the bond graph models, respectively.

And from the above equation, we can obtain [4]:

$$\dot{p}_2 = Se - \frac{R_s}{L_q} p_2 - \frac{K_e}{M} p_6 \qquad (20)$$

$$\dot{p}_6 = \frac{K_e}{L_q} p_2 - \frac{\mu}{M} p_6 \qquad (21)$$

$$f_6 = \frac{1}{M} p_6 \qquad (22)$$

From the control theory, the general state-space equation is:

$$\dot{x} = Ax + Bu \qquad (23)$$

$$y = Cx + Du \qquad (24)$$

Where $A = \begin{bmatrix} -\frac{R_s}{L_q} & -\frac{K_e}{M} \\ \frac{K_e}{L_q} & -\frac{\mu}{M} \end{bmatrix}$, $B = [1\ 0]^T$, $C = [0\ \frac{1}{M}]$, $D = 0$

C. Model Validation

The widely used transfer function of the PMLSM motor as described in [4], and can be derived from the equations described in [22] is as follows:

$$G(s) = \frac{\frac{3}{2} Ke}{(L_q s + R_s)(Ms + \mu) + \frac{3}{2} K_e^2} \qquad (25)$$

The coefficient $\frac{3}{2}$ is caused by the coordinate transformation, which is not essential for the principle of the PMLSM motor [4]. Therefore, the transfer function of the PMLSM motor can be described as follows:

$$G(s) = \frac{Ke}{(L_q s + R_s)(Ms + \mu) + K_e^2} \qquad (26)$$

To draw the block diagram of the equivalent model of the PMLSM motor, we used the bond graph equations and can be obtained as in [1] as follows:
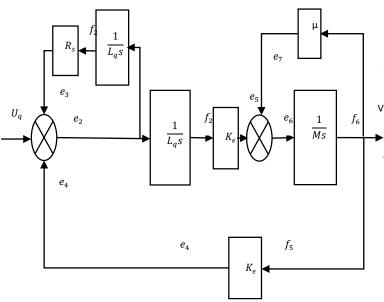
Figure 7 Block Diagram of PMLSM Model [1]

Reducing the above block diagram using the block diagram reduction technique, the transfer function of the PMLSM motor can be obtained as follows:
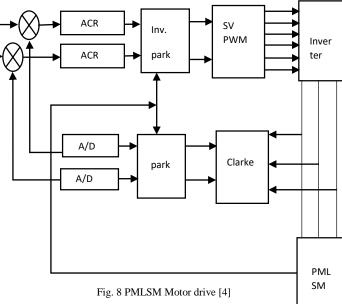
$$\frac{U_q(s)}{V(s)} = G(s) = \frac{Ke}{(L_q s + R_s)(Ms + \mu) + K_e^2} \qquad (27)$$

Therefore, equation 27 is the same as equation 26.

The transfer function of the PMLSM motor obtained from the bond graph model was validated by the block diagram was also simulated in 20 -SIM software in which a PI classical-based controller was developed to control the speed of the motor. The two PIs were developed: one is continuous, and the other is discrete for comparison purposes.
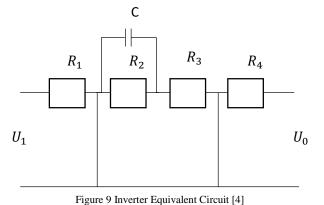
IV. PMLSM MOTOR DRIVE

The figure below shows the structure of the PMLSM motor, and its drives as adapted from [4]. The driver consists of the inverter, the analog to digital converters, the current regulator, and Pulse Width Modulation (PWM) generator.

Fig. 8 PMLSM Motor drive [4]

Therefore, the inverter can be represented by an equivalent circuit of two operational amplifiers, which is approximately ustrated in Fig. 9.
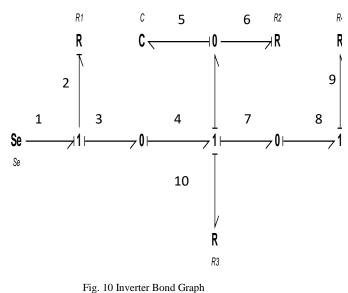
A. Inverter Bond Graph

Fig. 9 below shows the equivalent circuit of the inverter of the PMLSM motor. The circuit was obtained from an operational amplifier equivalent circuit that easily drives its bond graph model from the equivalent electric circuit model. However, the "current is collected by sensors in motor's winding, and the data subtract with the input

signal of i_q, then the current regulator output generates SVPWM waveform, finally the inverter drive A/B/C winding of PMLSM according to the SVPWM waveform" [4].

Figure 9 Inverter Equivalent Circuit [4]

Therefore, the bond graph model of the above inverter equivalent is obtained using 20-sim software. The motor

inverter, in this case, treated as a first-order inertia link with a time constant and equivalent current gain[4].

Fig. 10 Inverter Bond Graph

B. Mechanism Structure Bond Graph

The mechanism is generally represented by force moving a body of mass. The moving body plus the mass of the slider is represented by M_m as shown on the bond graph model in Fig. 10 below. therefore, the force of the PMLSM motor is related by the viscous friction as follows:

$$F = (M_m + M_L)\dot{v} + f(v) \qquad (28)$$

Therefore, the bond graph model of the equation above is obtained from 20-sim software as shown in Fig. 11. Therefore, it can be said that $M_m + M_L$ of equation 28 is

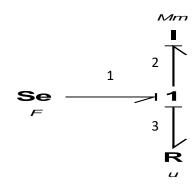represented by Mm on the bond graph model as shown in Fig. 11.

Fig. 11 Mechanism Bond Graph

C. PMLSM Drive System Bond Graph

Fig. 12 shows the bond graph model of the PMLSM motor drive system. The model was built in 20-sim software. The PMLSM motor drive system consists of the motor inverter, the motor, and the mechanism part.
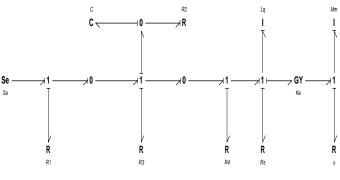

Figure 12 PMLSM Drive System Bond Graph

Therefore, the overall bond graph model of the PMLSM motor and its drive system was obtained by combining Fig. 6, Fig. 10, and Fig. 11 to form Fig. 12. Consequently, it can be said that the bond graph model of the PMLSM motor drive system is as shown by Fig. 12 above.

V. SIMULATION RESULTS

This section presents the results of the simulation of the bond graph model of the PMLSM motor and its drive presented in the previous sections. In the simulation model $R_s = 5.6\ \Omega$, $L_q = 1.8\ mH$, $K_e = 20\ N/A$, $M_m = 0.662\ kg$ in this case, the mass of the slider is 0.162 kg, and the load mass is 0.5 kg, making a total of 0.662 kg, and $U_{rms} = 150\ V$, $C = 241\mu F$. The time constant of the inverter is related by: $\tau = R_2 C$ and the amplifier gain is related by: $k = \frac{R_2}{R_1}$, $R_3 = R_4$, and $\mu = 0.00111$. These are the parameters that were used for simulations. The simulation was done based on the switching frequencies of the inverter and the resolutions as discussed. The global bond graph model of the PMLSM motor is developed. In this model, the resolution is used to analyze the model. The resolution is used when the power is

not considered. Therefore, in 20-sim software, the block diagram is combined with the bond graph model, and coupling is done with the aid of the sub-models [4]. The one junction for the bond graph model in the software is represented by the flow and used as the block diagram input. The one junction (the last one on the graph) is seen in Fig. 13 below. However, by means of a generator, the results of the block diagram can be converted into power. Therefore, the source of the flow of the bond graph of Fig. 12 is replaced by a modulated source of effort, as shown in Fig. 13.
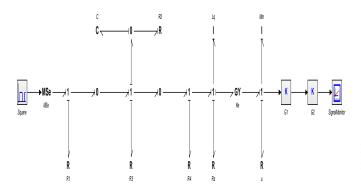

Figure 13 Global Model of the PMLSM

Fig. 13 above shows the global bond graph modeling and simulation of the PMLSM motor, and its drive system performed in 20-sim software. The input is tested by a square waveform, as shown.
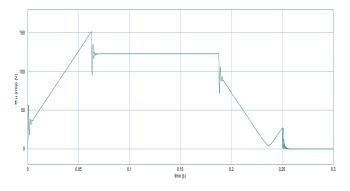

Fig. 14 RMS Voltage of the PMLSM

Fig. 14 above shows the simulated RMS voltage of the PMLSM motor as adapted. The simulated result was obtained from the dynamical simulation of the motor in the 20-sim software. The RMS voltage of the motor is 150 V.
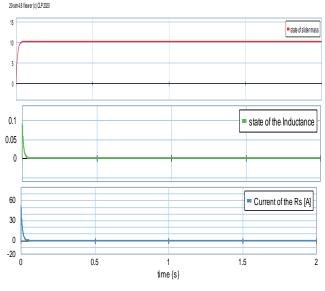

Figure 15 State of the Motor Parameters

Fig. 15 shows the state of the motor inductance and the load mass plus the mass of the slider of the PMLSM motor and the current through the motor series resistance.
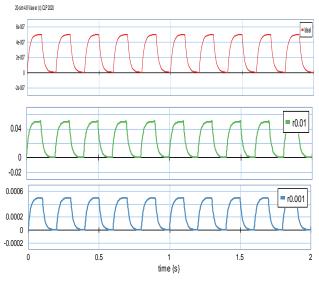

Figure 16 Drive Response due to Sensor Resolutions

Fig. 16 shows the motor response due to different sensor resolutions. An ideal condition is set which is in 'red,' and different values such as 0.01 and 0.001 were set, and they successfully followed the ideal case. A square test input was used, as seen from the global bond graph model in Fig. 12.
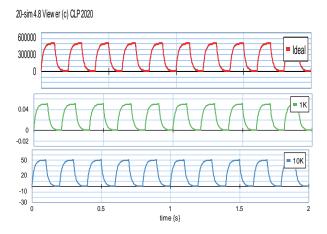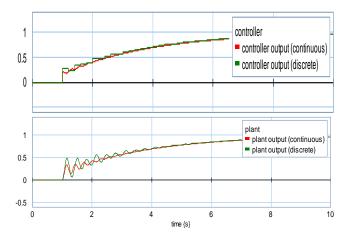
Fig. 17 Motor Response due to different Inverter Time Constants

Fig. 17 shows the response of the motor and drive system due to the different inverter time constants. The switching frequencies are 1 kHz and 10 kHz, respectively.

Fig. 18 PIs Speed Controls

Fig. 18 above showed the motor dynamical response when two classical PIs were implemented. The simulation results show that the controllers were successfully tracked the motor response. The two controllers implemented are discrete and continuous, respectively.

VI CONCLUSION

This paper has presented modeling, simulation, and control of the PMLSM motor for electric vehicle applications. The PMLSM motor is suitable for electric vehicles due to its high-power density and high efficiency. In addition, the bond graph model of the motor and its validation using block diagram and transfer function methods are also covered. The dynamical model obtained using bond graph proved to be the same model from the traditional differential and block diagram forms. Two classical PIs (discrete and continuous) were implemented to control the motor velocity due to a step input signal in 20-sim software. Both the controllers perfectly tracked velocity trajectories.

Moreover, the motor drive system, including the inverter, the drive mechanism, and the motor, were modeled and simulated using 20-sim software. The motor drive is responsible for its various industrial applications, especially for electric vehicles. The electric vehicle propulsion system depends on the motor power translated into the vehicle's movement. Therefore, this research ensures an effective inverter response to the motor to suit this application. Thus, the analysis was made based on the motor drive system response due to the different sensor resolutions and the inverter switching frequency.

REFERENCES

[1] L. Teng, L. Yanjie, and S. Lining, "Bond graph model of permanent magnet linear synchronous motor," in *2010 2nd International Conference on Industrial and Information Systems, IIS 2010*, 2010, vol. 2, pp. 128–131, DOI: 10.1109/INDUSIS.2010.5565660.

[2] J. Faiz and B. Rezaei-Alam, "Control of a Linear Permanent Magnet Synchronous Motor using Multiple Reference Frame Theory," in *The 17th International Conference on Magnetically Levitated Systems and Linear Drives*, 2002, no. January 2002.

[3] M. C. Sanchez and J. M. Larrahondo, "Permanent magnet synchronous linear motor for an urban transport electric vehicle," *Proc. - EMS 2015 UKSim-AMSS 9th IEEE Eur. Model. Symp. Comput. Model. Simul.*, pp. 301–306, 2016, DOI: 10.1109/EMS.2015.52.

[4] T. Li, Y. Liu, and L. Sun, "Global Model of PMLSM Drive System Using Bond," *Electr. Power Syst. Comput.*, pp. 615–622, 2011.

[5] R. Zrafi, S. Ghedira, and K. Besbes, "A bond graph approach for the modeling and simulation of a buck converter," *J. Low Power Electron. Appl.*, vol. 8, no. 1, 2018, DOI: 10.3390/jlpea8010002.

[6] A. Vaz, S. S. Dhami, and S. Trivedi, "Bond graph modeling and simulation of three phase PM BLDC motor," in *14th National Conference on Machines and Mechanisms, NaCoMM 2009*, 2020, pp. 1–6.

[7] C. Batlle and A. Dòria-Cerezo, "Bond graph models of electromechanical systems. The AC generator case," *IEEE Int. Symp. Ind. Electron.*, pp. 1064–1069, 2008, DOI: 10.1109/ISIE.2008.4677192.

[8] A. Grava, T. Maghiar, C. Grava, and Ş. Vasile, "The bond-graph analysis for the DC motor with

permanent magnets," 2017, no. July 2003.

[9] A. M. Mughal, "A Theoretical Framework for Modeling and Simulation with Optimal Control System of Voluntary Biomechanical Movements A Theoretical Framework for Modeling and Simulation with Optimal Control System of Voluntary Biomechanical Movements by Asif Mahmood Mugha."

[10] J. T. Machado, "Bond graph and memristor approach to DNA analysis," *Nonlinear Dyn.*, vol. 88, no. 2, pp. 1051–1057, 2017, DOI: 10.1007/s11071-016-3294-z.

[11] M. Zoheb and A. Mahmood, "Bond Graph Modeling and PID Controller Stabilization of Single Link Mechanical Model," 1938, no. October.

[12] A. M. Mughal and K. Iqbal, "Modelling and analysis physiological motor control using a bond graph," in *IFAC Proceedings Volumes (IFAC-PapersOnline)*, 2006, vol. 6, no. PART 1, pp. 393–398, DOI: 10.3182/20060920-3-fr-2912.00071.

[13] S. H. Abbasi and A. Mahmood, "Bond graph modeling of a customized anthropomorphic prosthetic hand with LQR control synthesis," in *Proceedings of 2017 International Multi-Topic Conference, INMIC 2017*, 2018, vol. 2018-Janua, no. November, pp. 1–6, DOI: 10.1109/INMIC.2017.8289466.

[14] R. Tapia-Sánchez, "Electrical Power Analysis Using the Scattering Bond Graph," *J. Eng. (United Kingdom)*, vol. 2015, 2015, DOI: 10.1155/2015/501747.

[15] A. K. Samantaray, K. Medjaher, B. O. Bouamama, M. Staroswiecki, and G. Dauphin-Tanguy, "Component-Based Modelling of Thermofluid Systems for Sensor Placement and Fault Detection," *Simulation*, vol. 80, no. 7–8, pp. 381–398, 2004, DOI: 10.1177/0037549704046339.

[16] W. Borutzky, "Bond graph modeling and simulation of mechatronic systems an introduction into the methodology," in *20th European Conference on Modelling and Simulation: Modelling Methodologies and Simulation Key Technologies in Academia and Industry, ECMS 2006*, 2006, pp. 17–28, DOI: 10.7148/2006-0017.

[17] P. J. Gawthrop and G. P. Bevan, "A tutorial introduction for control engineers," *IEEE Control Syst.*, vol. 27, no. 2, pp. 24–45, 2007, DOI: 10.1109/MCS.2007.338279.

[18] F. Azhar, H. Wakiwaka, K. Tashiro, and M. Nirei, "Design and performance index comparison of the permanent magnet linear motor," *Prog. Electromagn. Res. M*, vol. 43, no. November, pp. 101–108, 2015, DOI: 10.2528/PIERM15071204.

[19] N. A. Mohd Nasir, F. A. bin Abdul Shukor, R. N. Firdaus, H. Wakiwaka, K. Tashiro, and M. Nirei, "Design of the permanent magnet linear synchronous motor for high thrust and low cogging force performance," *Prog. Electromagn. Res. M*, vol. 63, no. January, pp. 83–92, 2018, DOI: 10.2528/pierm17101907.

[20] K. Divakar and N. R. Reddy, "Vector controlled PMLSM using simplified Space vector pulse width modulation," vol. 2, no. 3, pp. 1105–1110, 2012.

[21] T. Li, Q. Yang, and B. Peng, "Research on Permanent Magnet Linear Synchronous Motor Control System Simulation," in *AASRI Procedia*, 2012, vol. 3, pp. 262–269, DOI: 10.1016/j.aasri.2012.11.043.

[22] W. Te Su and C. M. Liaw, "Adaptive positioning control for an LPMSM drive based on the adapted inverse model and robust disturbance observer," *IEEE Trans. Power Electron.*, vol. 21, no. 2, pp. 505–517, 2006, DOI: 10.1109/TPEL.2005.869729.